EUROPEAN JOURNAL OF PURE AND APPLIED MATHEMATICS
2025, Vol. 18, Issue 4, Article Number 6691
ISSN 1307-5543 – ejpam.com
Published by New York Business Global

Impact of Awareness Programs on Whitefly Dynamics in Coconut Farming: A Unified DDE and SDE Modeling Approach

B. Dhivyadharshini[1], R. Senthamarai[1,*]

[1] *Department of Mathematics, College of Engineering and Technology, SRM Institute of Science and Technology, Kattankulathur-603203, Tamilnadu, India*

Abstract. In this article, we proposed a comprehensive pest control model that integrated both delay differential equations (DDEs) and stochastic processes to mitigate the spread of whiteflies in coconut plantations. The delay model introduced a time lag in the implementation of awareness programs and investigated its impact on the system's equilibrium stability. Numerical simulations validated the model's effectiveness in enhancing pest management. A stochastic component, formulated using a Wiener process within a system of non-linear ordinary differential equations (ODEs), was used to estimate the probability of disease elimination under environmental fluctuations. The study was novel in combining both deterministic delays and stochastic effects in a unified framework, offering deeper insights into timing and control efficiency. Although focused on coconut farming, the modeling approach and techniques had broader applicability in agricultural pest control scenarios. The findings enhanced our understanding of pest dynamics under uncertainty and delay, providing a foundation for more informed and effective control interventions in agricultural ecosystems.

2020 Mathematics Subject Classifications: 34A34, 92D45, 34K07, 34K20, 37H10, 65C30

Key Words and Phrases: Pest control model, farming awareness, delay differential equation, stochastic differential equation, numerical simulation

1. Introduction

Cocos nucifera, the coconut tree, is a vital crop with diverse benefits, from its nutrient-rich fruit to its versatile coir [1]. Coconut diseases impacted livelihoods, despite its antiviral properties; key components included endosperm (kernel), endocarp (shell), and mesocarp (coir) [2]. India, the third-largest producer, relied heavily on coconut-based industries, with products ranging from food and cosmetics to artistic crafts and eco-friendly materials [3]. This resilient palm provided antiviral properties, essential minerals, and economic

*Corresponding author.
DOI: https://doi.org/10.29020/nybg.ejpam.v18i4.6691

Email addresses: db0558@srmist.edu.in (B. Dhivyadharshini), senthamr@srmist.edu.in (R. Senthamarai)

sustainability [4]−[6]. Celebrated on World Coconut Day (September 2) [7], intercropping with floriculture enhanced farming efficiency [8], [9]. With applications in ropes, mats, insulation, and even rehydration therapy, the coconut truly embodied a functional, life-enriching resource [10]−[14].

The rugose spiraling whitefly (RSW), Aleurodicus rugioperculatus, first appeared in scientific literature in 2004 when Martin identified it and initially named it the gumbo limbo spiraling whitefly [15]. Highly polyphagous, it fed on over 118 hosts across 43 plant families. It was first detected in Tamil Nadu and Kerala in 2016 [16], RSW damaged coconut plantations by extracting nutrients, excreting honeydew, and promoting sooty mold growth, thereby reducing photosynthesis [17]. Infestation signs included egg spirals, white wax deposits, sticky honeydew, and black sooty mold [18]−[20]. Escalating infestations threatened coconut trees, emphasizing the need for farmer awareness to sustain production. Mathematical models helped analyze interacting populations, particularly in epidemiology, by revealing interactions and parameter impacts [21]. These models aided in understanding epidemic dynamics and control strategies [22], [23]. Studies on RSW infestations in coconut trees suggested that reducing the contact rate effectively controlled infection [24]. Awareness programs played a crucial role in promoting knowledge and understanding among farmers, leading to the adoption of improved agricultural practices, increasing productivity, and providing significant economic and social benefits to farming communities [25]. Research has explored media-driven vaccination awareness, farming awareness in pest control [26], [27]. The reproduction number, analyzed via the next-generation matrix, was found to be crucial in epidemiology [28].

A mathematical model represents real-world systems using variables, equations, and parameters to describe relationships and predict behavior under different conditions. Equilibrium points help analyze long-term dynamics [29]−[31]. DDEs incorporate time lags, making them suitable for systems where current changes depend on past states [32], [33]. Stochastic differential equations (SDEs) introduce randomness, accounting for uncertainty in system behavior [34]−[37]. Our study integrated DDEs and SDEs to model RSW infestations and awareness programs. Inspired by [38], [39], we extended the model in [40] with DDEs and SDEs to control RSW infestations and safeguard coconut populations through awareness programs. Our research is focused specifically on the Pollachi locality of Tamil Nadu. Thus, the parameter values were selected based on the same zone.

Section 2 begins with the development of the mathematical model, incorporating DDEs. It explores key properties such as positive invariance, boundedness, the basic reproduction number, and equilibrium analysis. The equilibrium analysis includes subsections on the tree-pest free equilibrium, pest-free equilibrium, and coexistence equilibrium, along with stability assessments under delay conditions. Section 3 introduces the SDE model, while Section 4 investigates parameter sensitivity. Section 5 presents results and discussion to validate the theoretical findings. Finally, Section 6 summarizes the key results and conclusions of the study.

2. Mathematical formulation of the problem

In [40], G. Suganya and R. Senthamarai studied the impact of awareness on the dynamics of pest control in coconut trees. Here, we have extended the ODE model to both DDE and SDE model. The tree population is classified into healthy trees H and infected trees E to evaluate the whitefly's effect on coconut trees. L refers to the population of whiteflies, and A indicates the number of awareness programs carried out over the time period t.

2.1. DDE model

We have added a time delay in the awareness programs within the system of equations, which impacts the infected tree density and whitefly density in efforts to control infectious diseases. The delayed model is given by:

The population of healthy coconut trees $H(t)$ grows logistically, reduced by infection from whiteflies with a Holling type II functional response. The logistic term accounts for total tree density (healthy plus infected) competing for site resources; specifically, parameter s denotes the plantation's tree density (see Table 1) and represents the total available resources (space, nutrients and light). Since infected trees, although reduced in health and productivity, remain physically present and continue to occupy space and consume resources, their presence contributes to the density-dependent limitation on healthy tree growth.

$$\frac{dH(t)}{dt} = rH(t)\left(1 - \frac{H(t)+E(t)}{s}\right) - \frac{\phi H(t)L(t)}{1+\gamma L(t)}. \tag{1}$$

The population of infected trees $E(t)$ increases by infections of healthy trees by whiteflies, modeled using a Holling type II functional response, and decreases due to natural mortality at rate k and awareness-driven control measures (with delay τ) at rate $bA(t-\tau)E(t)$. The awareness term $bA(t-\tau)E(t)$ represents the removal or recovery of infected trees through interventions such as roguing and replacement, which specifically target infected trees and not the vector population. In contrast, the whitefly population in Eq.(3) is affected by awareness through a separate term $vA(t-\tau)L(t)$, representing vector-specific control measures (e.g., pesticide application, biological control). Therefore, $bA(t-\tau)E(t)$ appears only in Eq.(2), while Eq.(3) includes its own awareness-related removal mechanism. Hence,

$$\frac{dE(t)}{dt} = \frac{\phi H(t)L(t)}{1+\gamma L(t)} - kE(t) - bA(t-\tau)E(t). \tag{2}$$

The whitefly population $L(t)$ is generated from infected trees at a per capita rate α, and declines through natural mortality at rate μ and awareness-mediated control actions that increase whitefly mortality after a delay. The term $vA(t-\tau)L(t)$ represents the reduction of the whitefly population due to awareness-driven interventions. Increased awareness (from $A(t-\tau)$) can lead to timely implementation of control strategies such as targeted pesticide application, release of natural predators, or improved sanitation of infested areas.

These measures directly reduce whitefly numbers rather than only indirectly affecting them through host removal; hence, the term is modeled as a direct mortality rate proportional to both $A(t-\tau)$ and the current whitefly density $L(t)$. Therefore,

$$\frac{dL(t)}{dt} = \alpha E(t) - \mu L(t) - vA(t-\tau)L(t). \tag{3}$$

The awareness variable $A(t)$ increases due to a baseline implementation of awareness programs and local reporting of infected trees, and decays over time in the absence of reinforcement. This dynamics is described by

$$\frac{dA(t)}{dt} = \delta + \beta E(t) - \xi A(t). \tag{4}$$

With the initial values

$$H(\theta) = l, \quad E(\theta) = m, \quad L(\theta) = n, \quad A(\theta) = q, \quad \theta \in [-\tau, 0]\,. \tag{5}$$

We assumed that $l > 0$, $m > 0$, $n > 0$, and $q > 0$ as these represent the initial positive population densities of healthy trees, infected trees, whiteflies, and the awareness level, respectively. This assumption ensured both the biological realism and the mathematical feasibility of the model. The same constant values l, m, n, q were assigned for $\theta \in [-\tau, 0]$ to represent a steady, uniform initial history before $t = 0$, implying no changes in the state variables during the delay period. This common assumption in delay differential equation models isolates the effect of the delay from additional variability in the initial conditions.

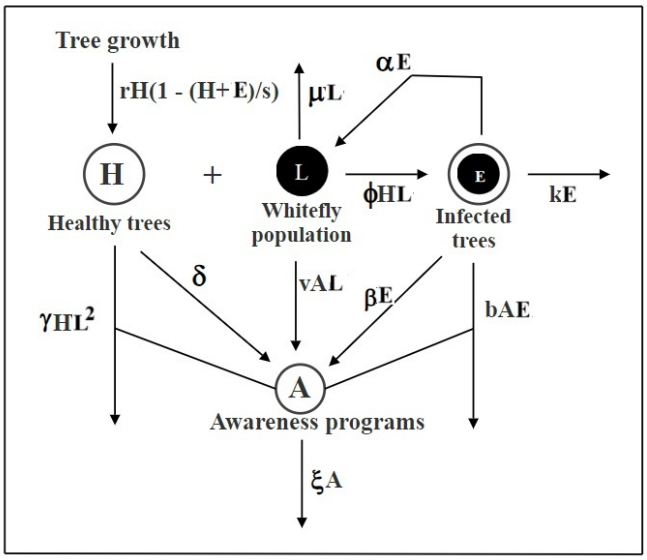

Figure 1: Schematic diagram

2.2. Positive invariance

The Eqs.(1) − (4) can be represented compactly as follows:

$$\frac{\mathrm{d}U}{\mathrm{d}t} = \Psi(U). \tag{6}$$

Here, let $U(\theta) = (H(\theta), E(\theta), L(\theta), A(\theta))^T \in C$, where $C = C\left([-\tau, 0], \mathbb{R}^4_+\right)$ represents the Banach space of continuous functions. The function $\Psi = (\Psi_1, \Psi_2, \Psi_3, \Psi_4)^T$ denotes the the right-hand terms in the system of Eqs.(1)−(4). Based on the fundamental theory of functional differential equations [41], a unique solution $(H(t), E(t), L(t), A(t))$ exists for the system described by Eqs.(1)−(4) given the initial conditions specified in Eq.(5).

Theorem 1. *All the solutions of Eqs.*(1)−(4) *with initial conditions Eq.*(5) *are positive.*

Proof. This theorem was validated by the method described in [42] and [43]. Indeed, it is straightforward to verify in Eqs.(1) − (4) that anytime determining $H(\theta) \in R_+$ with $H = 0$, $E = 0$, $L = 0$, $A = 0$. Then

$$\Psi_i(U) \mid_{U_i=0, U\in R^4_+} \geq 0.$$

Using Lemma 2 from [43] and Theorem 1.1 from [42], any solution $x(t) = x(t, x(\theta))$ of Eqs.(1) − (4) with $x(\theta) \in C$ is such that $U(t) \in R^4_+$ for all $t \geq 0$. Since all solutions to Eqs. (1) − (4) are non - negative for any $t > 0$, we can deduce that the solution lies in the region R^4_+. Consequently, the positive cone $\mathbb{R}^4_+$ serves as an invariant region.

2.3. Boundedness

Boundedness in a system reflects its proper behavior, as it guarantees that none of the interacting sub populations can rise to infinity in a finite amount of time.
If we define $N = H + E$ to be the total plant biomass at any time t, then combining the Eqs.(1) and (2) results in:

$$\frac{\mathrm{d}N}{\mathrm{d}t} = rE\left[1 - \frac{H+E}{s}\right] - kE - bA(t-\tau)E \leq rN\left(1 - \frac{N}{s}\right),$$

thus, it follows

$$\lim_{t\to\infty} \sup N \leq M := \max\{N(0), s\}.$$

Similarly, taking into account the aware population, we get

$$\frac{\mathrm{d}A}{\mathrm{d}t} = \delta + \beta E - \xi A \leq \delta + \beta E - \eta A,$$

giving again an upper bound

$$\lim_{t\to\infty} \sup A \leq \frac{\delta + \beta s}{\eta}.$$

Again,

$$\frac{\mathrm{d}L}{\mathrm{dt}} = \alpha E - \mu L - vA(t-\tau)L \leq \alpha s - \mu L,$$

and it follows

$$\lim_{t\to\infty} \sup L \leq \frac{\alpha s}{\mu}.$$

Thus, the set determines the region of attraction

$$\mathcal{D} = \left\{ (H, E, L, A) \in \mathbb{R}^4_+ : 0 \leq H + E \leq M, 0 \leq L \leq \frac{\alpha s}{\mu}, 0 \leq A \leq \frac{\delta + \beta s}{\eta} \right\},$$

which attracts all solutions from the positive cone's interior and is positively invariant.

2.4. Reproduction number

At pest-free equilibrium, when $\tau = 0$, the disease class Eqs.(2) and (3) characterize the population inputs in terms of the population size and the initial number of infections. The reproduction number is derived using the next-generation matrix approach introduced by Diekmann et al. [44].

$$R_0 = \frac{\phi s \alpha\, \xi^2}{(\xi k + b\delta)(\mu\xi + v\delta)}.$$

The product $\phi s\alpha$ in the numerator captures the combined effects of transmission from whiteflies to healthy trees (ϕs) and the production of new whiteflies by infected trees (α). The factor ξ^2 arises from substituting the pest-free awareness level $A^* = \delta/\xi$ into the next-generation matrix formulation, reflecting the role of awareness decay in both host and vector components. The denominator $(\xi k + b\delta)(\mu\xi + v\delta)$ represents the effective removal rates of infected trees and whiteflies, combining natural mortality with awareness-driven control actions.

2.5. Equilibria and stability assessment of delayed system

The following matrix form represents the linearization of the system defined by Eqs.(1)−(4):

$$\frac{d}{dt}\begin{bmatrix} H(t) \\ E(t) \\ L(t) \\ A(t) \end{bmatrix} = F \begin{bmatrix} H(t) \\ E(t) \\ L(t) \\ A(t) \end{bmatrix} + G \begin{bmatrix} H(t-\tau) \\ E(t-\tau) \\ L(t-\tau) \\ A(t-\tau) \end{bmatrix},$$

where F and G are,

$$F = \begin{bmatrix} r - \frac{r(2H+E)}{s} - \frac{\phi L}{1+\gamma L} & -\frac{rH}{s} & -\frac{\phi H}{(1+\gamma L)^2} & 0 \\ \frac{\phi H}{1+\gamma L} & -k & \frac{\phi H}{(1+\gamma L)^2} & 0 \\ 0 & \alpha & -\mu & 0 \\ 0 & \beta & 0 & -\xi \end{bmatrix}, \quad G = \begin{bmatrix} 0 & 0 & 0 & 0 \\ 0 & 0 & 0 & -bE \\ 0 & 0 & 0 & -vL \\ 0 & 0 & 0 & 0 \end{bmatrix}. \quad (7)$$

Table 1: Model parameters and their corresponding values.

Symbol	**Meaning**	**Unit**	**Value used for analysis** [40]	**Range** [40]
s	Tree density	acre^{-1}	70	$60-70$
r	Replanting rate	day^{-1}	0.0005	$0-0.003$
k	Mortality rate of tree	day^{-1}	0.0002	$0-0.002$
ϕ	Contact rate	$\text{pest}^{-1}\text{day}^{-1}$	0.0002	$0-0.002$
α	Whitefly birth rate	day^{-1}	0.2	$0.1-0.3$
μ	Death rate of whitefly	day^{-1}	0.06	$0.06-0.1$
γ	Saturation constant	–	0.2	0.2
b	Maximum activity rate	day^{-1}	0.0001	$0-0.0001$
v	Death rate of whitefly due to awareness	day^{-1}	0.005	0.005
δ	Rate of awareness programs	day^{-1}	0.03	0.03
β	Rate of local awareness	day^{-1}	0.025	0.025
ξ	Fading rate of awareness	day^{-1}	0.015	0.015

The characteristic equation of the system can be written as

$$\Upsilon(\sigma) = \mid \sigma I - F - e^{-\sigma\tau}G \mid = 0. \tag{8}$$

The system's equilibrium points can be represented as:

(i) Tree−pest free equilibrium: $E_0 = (0, 0, 0, \frac{\delta}{\xi})$,

(ii) Pest−free equilibrium: $E_1 = (s, 0, 0, \frac{\delta}{\xi})$,

(iii) Coexistence equilibrium: $\bar{E} = (H^*, E^*, L^*, A^*)$,

where,

$$H^* = (k + bA^*)\frac{\beta(\mu + vA^*) + \gamma\alpha(\xi A^* - \delta)}{\phi\beta\alpha}, \quad E^* = \frac{\xi A^* - \delta}{\beta}, \quad L^* = \frac{\alpha(\xi A^* - \delta)}{\beta(\mu + vA^*)}.$$

The coexistence equilibrium is determined by the positive root A^* of the cubic equation

$$p_3A^3 + p_2A^2 + p_1A + p_0 = 0, \tag{9}$$

where the coefficients p_i are algebraic combinations of model parameters:

$$\begin{aligned}
p_3 &= rb\mu\gamma v\beta + rb\gamma^2\xi^2,\\
p_2 &= rk\beta\gamma\xi v + rk\gamma^2\alpha\xi^2 + rb\beta^2v\mu + rb\mu\xi\gamma\beta - rb\mu\gamma\delta\beta v + r\gamma\phi\alpha\xi^2 + rb\gamma\xi\alpha\beta,\\
p_1 &= rk\mu\gamma\xi\beta + rk\beta^2v + rk\gamma\alpha\xi\beta + rb\mu\beta^2 + rb\gamma^2\alpha\delta^2 + \xi r\phi\beta\alpha - rs\phi\alpha\xi\gamma\\
&\quad - rk\beta^2v\gamma\delta - 2rk\gamma^2\alpha\xi\delta - rb\mu\delta\gamma\beta - rb\gamma\alpha\delta\beta - \xi r\phi\alpha\gamma\delta - r\delta\alpha\phi\gamma\xi,\\
p_0 &= rs\phi\beta\alpha\gamma\delta + rk\mu\beta^2 - rk\mu\gamma\delta\beta - rs\phi\beta^2\alpha - rk\gamma\alpha\delta\beta + rk\gamma^2\alpha\delta^2\\
&\quad - rk\phi\beta\alpha + r\delta^2\gamma\phi\alpha + s\delta\phi^2\beta\alpha.
\end{aligned}$$

The biologically admissible root must satisfy

$$A^* > \frac{\delta}{\xi},$$

so that $E^* > 0$. Among the real roots, we selected the unique value fulfilling this condition as the biologically meaningful equilibrium for subsequent stability and simulation analyses.

2.5.1. Stability analysis at the tree–pest free equilibrium: $E_0 = \left(0, 0, 0, \frac{\delta}{\xi}\right)$

Lemma 1. The tree–pest free equilibrium E_0 is always unstable [24].

Proof. At E_0, the Jacobian matrix of the system has at least one eigenvalue with a positive real part for all biologically admissible parameter values. This implies that any small perturbation from E_0, such as the introduction of a small number of whiteflies or infected trees, will grow over time. Biologically, in the absence of healthy and infected trees as well as pests, the introduction of pests leads to growth due to the lack of competition and absence of control measures. Hence, E_0 is unstable for all parameter values.

2.5.2. Stability analysis at the pest−free equilibrium: $E_1 = \left(s, 0, 0, \frac{\delta}{\xi}\right)$

By substituting the equilibrium point into the matrices presented in Eq.(7), we can derive F and G:

$$F = \begin{bmatrix} -r & -r & -\phi s & 0 \\ \phi s & -k & \phi s & 0 \\ 0 & \alpha & -\mu & 0 \\ 0 & \beta & 0 & -\xi \end{bmatrix}, \quad G = \begin{bmatrix} 0 & 0 & 0 & 0 \\ 0 & 0 & 0 & 0 \\ 0 & 0 & 0 & 0 \\ 0 & 0 & 0 & 0 \end{bmatrix}. \tag{10}$$

Substituting F and G in Eq.(8), the transcendental equation derived from the matrix is

$$\psi(\sigma, \tau) = \sigma^4 + A_1\sigma^3 + A_2\sigma^2 + A_3\sigma + A_4 = 0, \tag{11}$$

with coefficients:

$$\begin{aligned} A_1 &= k + \mu + r + \xi, \\ A_2 &= k\mu - \alpha\phi s + kr + \mu r + \phi rs + k\xi + \xi\mu + r\xi, \\ A_3 &= \alpha\phi^2 s^2 - \alpha\phi rs + k\mu r + \mu\phi rs - \alpha\phi s\xi + k\mu\xi + kr\xi + \mu r\xi + \phi rs\xi, \\ A_4 &= \alpha\phi^2 - \alpha\phi rs\xi + k\mu r\xi + \mu\phi rs\xi. \end{aligned}$$

Theorem 2. *The pest free equilibrium E_1 is locally asymptotically stable (LAS) for $R_0 < 1$ and unstable otherwise.*

Proof. At E_1, the system is locally asymptotically stable if it satisfies the Routh–Hurwitz conditions:

$$A_4 > 0, \quad A_1A_2 - A_3 > 0, \quad \text{and} \quad (A_1A_2 - A_3)A_3 - A_1^2A_4 > 0.$$

These inequalities hold precisely when $R_0 < 1$, ensuring E_1 is locally asymptotically stable; otherwise, it is unstable.

2.5.3. Stability analysis at the Coexistence equilibrium: $\bar{E} = (H^*, E^*, L^*, A^*)$

When we substitute the equilibrium point into the matrices from Eq.(7), we obtain F and G:

$$F = \begin{bmatrix} r - \frac{r(2H^*+E^*)}{s} - \frac{\phi L^*}{1+\gamma L^*} & -\frac{rH^*}{s} & -\frac{\phi H^*}{(1+\gamma L^*)^2} & 0 \\ \frac{\phi H^*}{1+\gamma L^*} & -k & \frac{\phi H^*}{(1+\gamma L^*)^2} & 0 \\ 0 & \alpha & -\mu & 0 \\ 0 & \beta & 0 & -\xi \end{bmatrix}, \quad G = \begin{bmatrix} 0 & 0 & 0 & 0 \\ 0 & 0 & 0 & -bE^* \\ 0 & 0 & 0 & -vL^* \\ 0 & 0 & 0 & 0 \end{bmatrix}. \tag{12}$$

Substituting F and G in Eq.(8), the transcendental equation derived from the matrix is,

$$\psi(\sigma, \tau) = \sigma^4 + A_1\sigma^3 + A_2\sigma^2 + A_3\sigma + A_4 + e^{-\sigma\tau}[B_1\sigma^2 + B_2\sigma + B_3] = 0, \tag{13}$$

with coefficients:

$$\begin{aligned}
A_1 &= \xi + \mu + k - r + \frac{r(2H^* + E^*)}{s}, \\
A_2 &= \mu\xi + k\xi + k\mu - \frac{\phi H^* \alpha}{(1+\gamma L^*)^2} - r\xi - r\mu - rk + \frac{r(2H^* + E^*)\xi}{s} + \frac{r(2H^* + E*)\mu}{s} \\
&+ \frac{r(2H^* + E^*)k}{s} + \frac{rH^{2*}\phi}{s(1+\gamma L^*)} + \frac{\phi^2 H^{2*}}{(1+\gamma L^*)^3}, \\
A_3 &= \mu k\xi - \frac{\phi H^* \alpha\xi}{(1+\gamma L^*)^2} - \frac{\phi H^* \beta v L^*}{(1+\gamma L^*)^2} - r\mu\xi - rk\xi - rk\mu + \frac{r\phi H^* \alpha}{(1+\gamma L^*)^2} \\
&+ \frac{r(2H^* + E^*)\mu\xi}{s} + \frac{r(2H^* + E^*)k\xi}{s} + \frac{r(2H^* + E^*)k\mu}{s} \\
&- \frac{r(2H^* + E^*)(\phi H^* \alpha)}{s(1+\gamma L^*)^2} + \frac{rH^{2*}\phi\xi}{s(1+\gamma L^*)} + \frac{rH^{2*}\phi\mu}{s(1+\gamma L^*)} + \frac{\phi H^* \xi}{1+\gamma W^*}, \\
A_4 &= \frac{\phi r H^* \alpha\xi}{(1+\gamma L^*)^2} - r\mu k\xi - \frac{r(2H^* + E^*)\phi H^* \alpha\xi}{s(1+\gamma L^*)^2} - \frac{r(2H^* + E^*)\phi H^* \alpha\xi}{s(1+\gamma L^*)^2} \\
&+ \frac{rH^{2*}\phi\mu\xi}{s(1+\gamma L^*)}, \\
B_1 &= -bE^*\beta, \\
B_2 &= rbE^*\beta - bE^*\beta\mu - \frac{r(2H^* + E^*)bE^*\beta}{s}, \\
B_3 &= \frac{\phi r H^* \beta v L^*}{(1+\gamma L^*) + rbE^*\beta\mu} - \frac{r(2H^* + E^*)bE^*\beta\mu}{s} + \frac{\phi H^* \beta v L^*}{(1+\gamma L^*)}.
\end{aligned} \tag{14}$$

In the presence of τ, determining root signs was challenging. We knew that $\bar{E}$ was locally asymptotically stable if all its characteristic equation roots had negative real parts. When a root had a positive real part, the system became unstable. If all roots were imaginary, stability switches occurred. The transcendental Eq. (13) possessed an infinite number of

complex roots, in which the coefficients B_1, B_2, and B_3 arose from the delay-dependent part of the characteristic equation and were multiplied by the exponential term $e^{-\sigma\tau}$, explicitly capturing how τ influenced stability through delayed reproduction, mortality, and maturation effects. Biologically, B_1 reflected the influence of delayed reproduction on system inertia, B_2 described how delayed feedback altered mortality and transition rates, and B_3 captured the direct impact of delayed maturation and reproduction on growth dynamics. Large absolute values of these coefficients indicated greater sensitivity of the coexistence equilibrium to delays, potentially leading to destabilization and sustained oscillations when τ exceeded critical thresholds. To handle the infinite number of roots arising from the exponential terms, we followed the standard approach for delay differential equations: we first set the delay to zero to establish baseline stability, then considered purely imaginary roots ($\sigma = i\omega$) by separating the real and imaginary parts of Eq.(13) to solve for ω and τ. This allowed us to determine the critical delay values at which a pair of complex conjugate roots crossed the imaginary axis, indicating a Hopf bifurcation, and to deduce stability for τ below and above these thresholds without computing the full infinite spectrum.

Case I: when $\tau = 0$

Theorem 3. *The coexistence equilibrium point $\bar{E}$ is stable if the following conditions are satisfied, where the relevant quantities are defined in the proof below:*

$$A_4 > 0, A_1A_2 - A_3 > 0, (A_1A_2 - A_3)A_3 - A_1^2A_4 > 0. \tag{15}$$

Proof.

Without the delay, the characteristic Eq.(13) simplifies to:

$$\sigma^4 + A_1\sigma^3 + (A_2 + B_1)\,\sigma^2 + (A_3 + B_2)\,\sigma + (A_4 + B_3) = 0. \tag{16}$$

Eq.(16) with coefficients in Eq.(14) has negative or imaginary roots with negative real parts, provided the Routh–Hurwitz conditions in Eq.(15) are satisfied, making the system stable.

Case II: when $\tau > 0$

In this case, Eq.(13) possesses infinitely many roots. Stability requires roots of the characteristic Eq.(13) with negative real parts. Stability changes of $\bar{E}$ happens when the characteristic Eq.(13) possesses purely imaginary solutions. Consider a root of Eq.(13) to be $i\omega$. So we get

$$\omega^4 - A_2\omega^2 + A_4 = \left[-\omega^2 B_1 - B_3\right]\cos\omega\tau - [\omega B_2]\sin\omega\tau, \tag{17}$$

$$A_1\omega^3 - A_3\omega = \left[-\omega^2 B_1 - B_3\right]\sin\omega\tau - [\omega B_2]\cos\omega\tau. \tag{18}$$

Squaring and adding the two above mentioned equations

$$\omega^8 + \zeta_1\omega^6 + \zeta_2\omega^4 + \zeta_3\omega^2 + \zeta_4 = 0. \tag{19}$$

Substituting $\omega^2 = \ell$ in Eq.(19), introduced to simplify the stability analysis with respect to the delay parameter τ. This transformation reduces the degree of the characteristic equation from being in terms of ω^8 (Eq. (19)) to a quartic equation in ℓ (Eq. (20)). A quartic form is easier to handle analytically and allows direct application of the Routh–Hurwitz criterion to determine stability. Additionally, since ω^2 is always non-negative for real ω, working with ℓ eliminates the need to separately track positive and negative frequency roots, making it straightforward to assess stability changes and detect the onset of purely imaginary roots.

$$\ell^4 + \lambda_1\ell^3 + \lambda_2\ell^2 + \lambda_3\ell + \lambda_4 = 0, \tag{20}$$

where

$$\lambda_1 = A_1^2 - 2A_2, \quad \lambda_2 = A_2^2 + 2A_4 - 2A_1A_3 - 2B_1^2,$$
$$\lambda_3 = A_3^2 - 2A_2A_4 - 4B_1B_3 - 2B_2^2, \quad \lambda_4 = A_4^2 + 2B_3^2.$$

Eq.(20) exhibits roots with negative real parts if and only if the Routh-Hurwitz condition in Eq.(21) holds true. In this case, for the roots we find $\omega_k^2 = \ell_k < 0$, implying that the roots of Eq.(13) are real, $i\omega_k = \mp\sqrt{\ell_k}$, rather than purely imaginary. In summary, we have the theorem and it is stated as follows.

Theorem 4. *In case of the delayed model Eq.*(13)*, the endemic steady-state $\bar{E}$ is locally asymptotically stable for all $\tau > 0$, if the following conditions are satisfied:*

$$\lambda_1 > 0, \quad \lambda_4 > 0, \quad \lambda_1\lambda_2 - \lambda_3 > 0, \quad (\lambda_1\lambda_2 - \lambda_3)\,\lambda_3 - \lambda_1^2\lambda_4 > 0. \tag{21}$$

Proof.

Instead, if $\lambda_4 < 0$, Eq.(20) has at least one positive root $\omega_0 > 0$. We find that $\pm i\sqrt{\omega_0}$ is a root of Eq.(13) for the delay τ^*. By Butler's lemma given in [45], the endemic equilibrium $\bar{E}$ is stable when $\tau < \tau^*$, which is a critical delay value for the delayed system of Eqs.(1)-(4) remains stable. Using Eq.(17), we can determine

$$\begin{aligned}\cos\omega\tau &= \frac{1}{\triangle}\begin{vmatrix} D_1\omega^4 - A_2\omega^2 + A_4 & -\omega B_2 \\ A_1\omega^3 - A_3\omega & -\omega^2 B_1 - B_3 \end{vmatrix},\\ &= -\omega^6 B_1 - \omega^4 B_3 + A_2\omega^4 B_1 + A_2 B_3\omega^2 - \omega^2 A_4 B_1 - A_4 B_3\\ &+\phi^4 B_2 A_1 - \omega^2 A_3 B_2, \end{aligned} \tag{22}$$

where

$$\begin{aligned}\triangle &= \begin{vmatrix} -B_1 & B_2\omega \\ B_2\omega & B_1 \end{vmatrix},\\ &= B_1^2 + B_2^2\omega^2 > 0.\\ \sin\omega\tau &= \frac{1}{\triangle}\begin{vmatrix} -\omega^2 B_1 - B_3 & \omega^4 - A_2\omega^2 + A_4 \\ -\omega B_2 & A_1\omega^3 - A_3\omega \end{vmatrix},\\ &= -\omega^5 B_1 A_1 + \omega^3 B_1 A_3 - B_3 A_1\omega^3 + A_3 B_3\omega + \omega^5 B_2 \end{aligned}$$

$$-A_2B_2\omega^3 + \omega B_2A_4, \tag{23}$$

where

$$\begin{aligned}\triangle &= \begin{vmatrix} -\omega^2B_1 - B_3 & -\omega B_2 \\ -\omega B_2 & -\omega^2B_1 - B_3 \end{vmatrix}, \\ &= [\omega^2B_1 + B_3]^2 - \omega^2B_2^2. \end{aligned} \tag{24}$$

$$\tau^* = \frac{1}{\omega_0}\cos^{-1}\left(\frac{N_C(\omega_0)}{\Delta(\omega_0)}\right) + \frac{2\pi n}{\omega_0}, \quad n = 0, 1, 2, \ldots \tag{25}$$

where,

$$\Delta(\omega) = \left[\omega^2B_1 + B_3\right]^2 - \omega^2B_2^2,$$

$$N_C(\omega) = -\omega^6B_1 - \omega^4B_3 + A_2\omega^4B_1 + A_2B_3\omega^2 - \omega^2A_4B_1 - A_4B_3 + \phi^4B_2A_1 - \omega^2A_3B_2.$$

The set of ordered pair is (ω_0, τ^*). Additionally, we can confirm that the following transversality requirement:

$$\frac{d}{dt}Re\lambda\,(\tau)||_{\tau=\tau^*} = \frac{d}{dt}\eta\,(\tau)\Big|_{\tau=\tau^*} > 0. \tag{26}$$

This condition is satisfied. Owing to continuity, the real part of $\lambda\,(\tau)$ becomes positive once $\tau > \tau^*$ resulting in an unstable steady state. This indicates a bifurcation occurring at $\tau = \tau^*$, as demonstrated by Eqs.(1)−(4).

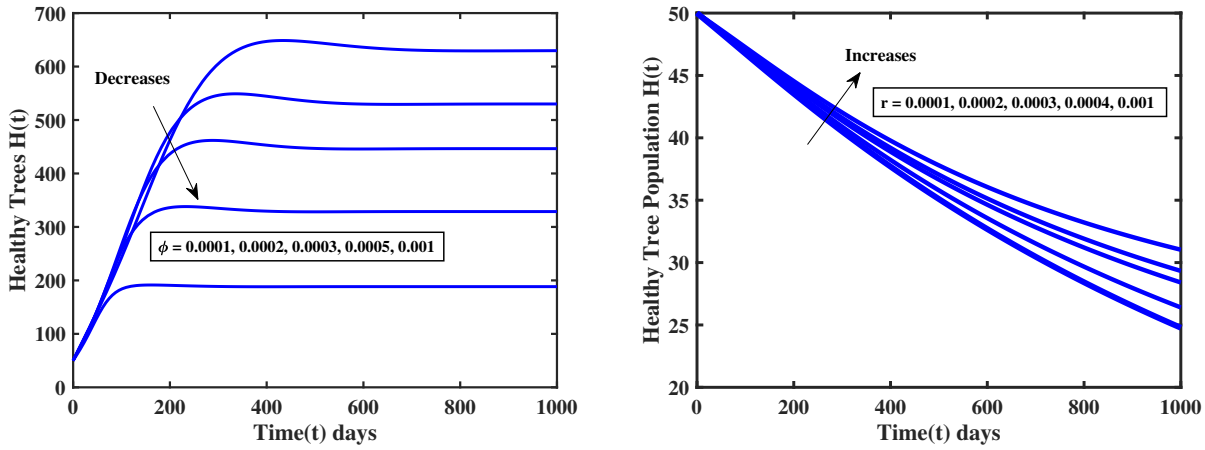

(a) (b)

Figure 2: Healthy tree profile $H(t)$ versus time (1000 days) in the presence of a time delay $\tau = 0.5$ (a) for various values of contact rate ϕ (b) for various values of replanting rate r with other parameters held at their fixed values.

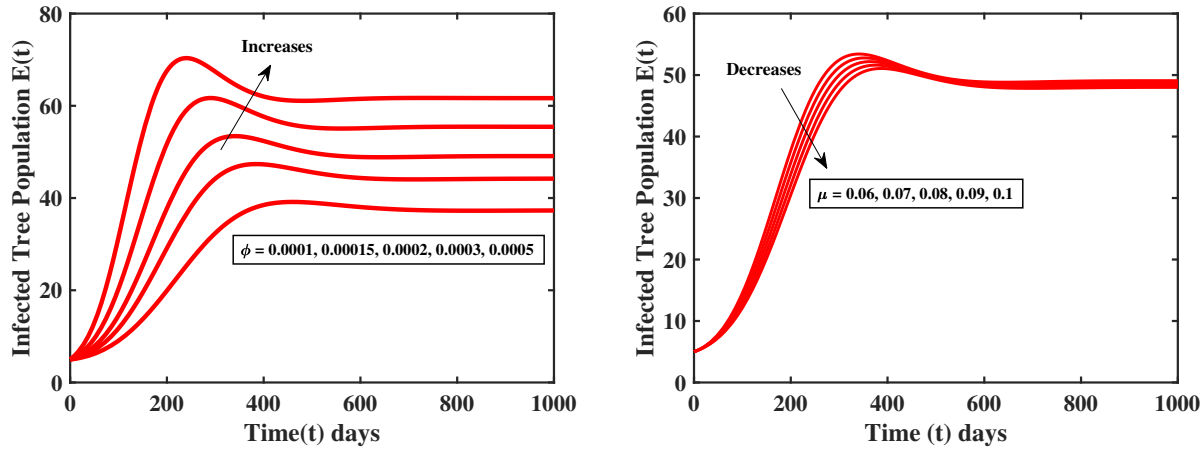

(a) (b)

Figure 3: Infected tree profile $E(t)$ versus time (1000 days) in the presence of a time delay $\tau = 0.5$ (a) for various values of contact rate ϕ, (b) for various values of death rate of whitefly μ with other parameters held at their fixed values.

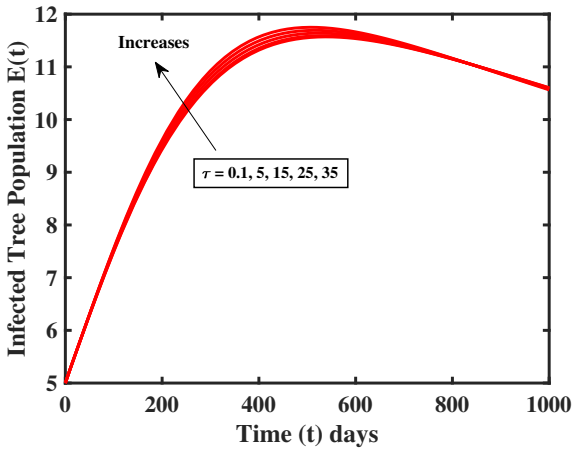

(a)

Figure 4: Infected tree profile $E(t)$ versus time (1000 days) in the presence of a time delay $\tau = 0.5$ (a) for various values of time delay parameter τ with other parameters held at their fixed values.

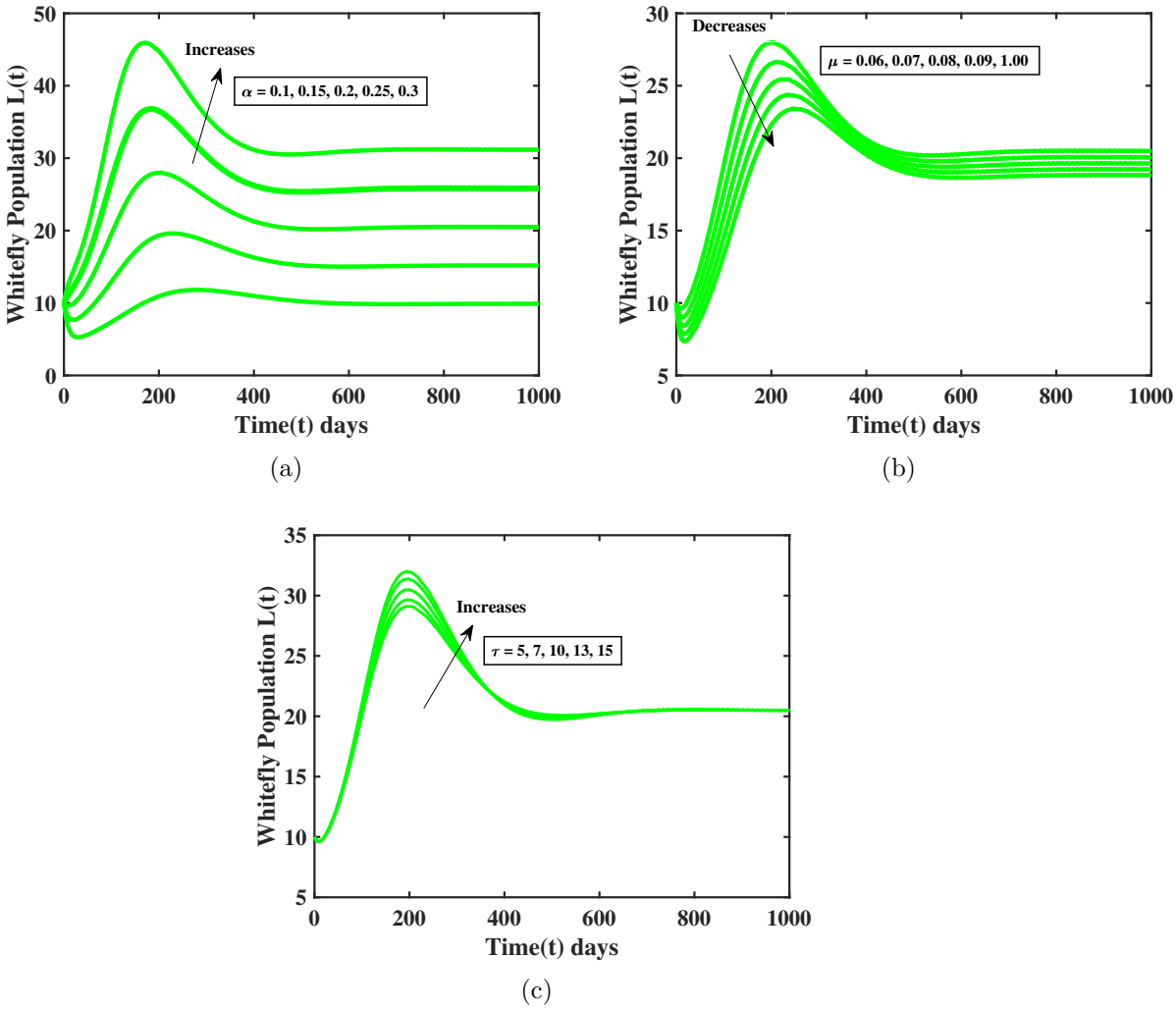

Figure 5: Whitefly profile $L(t)$ versus time (1000 days) in the presence of a time delay $\tau = 0.5$ (a) for various values of its birth rate α, (b) for various values of death rate μ, (c) for various values of time delay parameter τ with other parameters held at their fixed values.

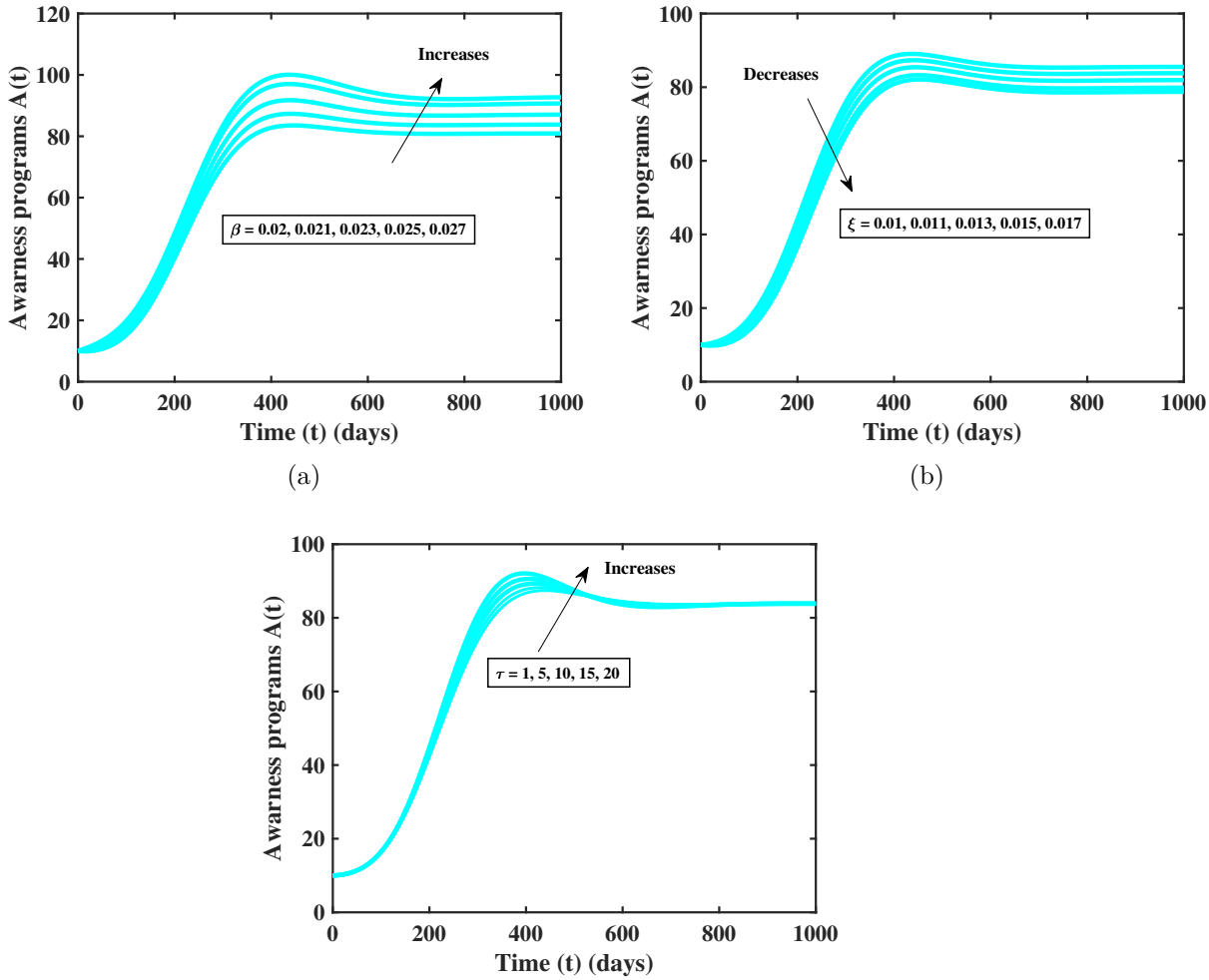

Figure 6: Awareness programs profile A(t) versus time (1000 days) in the presence of a time delay $\tau = 0.5$ (a) for various values of its local awareness rate β, (b) for various values of fading away rate ξ, (c) for various values of time parameter τ with other parameters held at their fixed values.

3. SDE model

ODE models have limitations, as real biological systems are often influenced by factors that are difficult to predict or quantify. Therefore, it is necessary to enhance these models to include more complex models that can capture the variability in biological dynamics. Consequently, understanding randomness as a key factor in the evolution of biological systems under stochastic influences is crucial. Here, we built an SDE model by

expanding the ODE model with the addition of stochastic processes to the derived system equations.The text below outlines our approach to deriving an SDE model from the ODE model, using the method introduced by Yuvan et al. [46].
Let $X(t) = (X_1(t), X_2(t), X_3(t), X_4(t))^T$ be a continuous random variable corresponding to $(H(t), E(t), L(t), A(t))^T$, where T denotes the transpose of a matrix. Additionally, let represent the random vector capturing the changes in the random variables over the time interval $\triangle t$. Every possible change between states in the SDE model is represented by the transition map. Based on ODE model in [40], there are 13 possible state changes that can occur within a small time interval $\triangle t$. Table 2 provides an overview of the state changes along with their associated probabilities. As an example, if one tree gets infected by whiteflies, the corresponding state change $\triangle X$ is expressed as $\triangle X = (-1, 1, 0, 0)$ and the probability of this change can be calculated using Table 2. $\triangle X = X(t+\triangle t) - X(t) =$

Table 2: Possible state changes and their corresponding probabilities.

Possible State Change	**Probability of State Change**
$(\Delta X)_1 = (-1, 1, 0, 0)^T$: Healthy trees interact with whiteflies and turn into infected trees	$P_1 = \phi X_1 X_3 \triangle t + o(\triangle t)$
$(\Delta X)_2 = (0, -1, 0, 0)^T$: Natural death of infected trees	$P_2 = kX_2 \triangle t + o(\triangle t)$
$(\Delta X)_3 = (0, 0, 1, 0)^T$: Spread of whiteflies from infected trees	$P_3 = \alpha X_2 \triangle t + o(\triangle t)$
$(\Delta X)_4 = (0, -1, 0, 0)^T$: Eradication of infected trees by awareness programs	$P_4 = bX_4 X_2 \triangle t + o(\triangle t)$
$(\Delta X)_5 = (-1, 0, 0, 0)^T$: Eradication of healthy trees by awareness programs	$P_5 = \gamma X_1 X_3^2 \triangle t + o(\triangle t)$
$(\Delta X)_6 = (0, 0, 0, 1)^T$: Awareness programs initiated by uninfected trees	$P_6 = \delta \triangle t + o(\triangle t)$
$(\Delta X)_7 = (0, 0, 0, 1)^T$: Awareness programs initiated by infected trees	$P_7 = \beta X_2 \triangle t + o(\triangle t)$
$(\Delta X)_8 = (0, 0, -1, 0)^T$: Natural death of whiteflies	$P_8 = \mu X_3 \triangle t + o(\triangle t)$
$(\Delta X)_9 = (0, 0, 0, -1)^T$: Awareness programs fade over time	$P_9 = \xi X_4 \triangle t + o(\triangle t)$
$(\Delta X)_{10} = (1, 0, 0, 0)^T$: Growth of healthy trees (logistic model)	$P_{10} = rX_1 \triangle t + o(\triangle t)$
$(\Delta X)_{11} = (-1, 0, 0, 0)^T$: Death of healthy trees (logistic model)	$P_{11} = \left(\frac{rX_1(X_1+X_2)}{s}\right) \triangle t + o(\triangle t)$
$(\Delta X)_{12} = (1, 0, 0, -1)^T$: Death of whiteflies due to awareness programs	$P_{12} = \mu X_3 \triangle t + o(\triangle t)$
$(\Delta X)_{13} = (0, 0, 0, 0)^T$: No change in state	$P_{13} = 1 - \sum_{i=1}^{12} P_i + o(\triangle t)$

$(\triangle X_1, \triangle X_2, \triangle X_3, \triangle X_4)$ Prob{ $(\triangle X_1,\ \triangle X_2,\ \triangle X_3,\ \triangle X_4)$ =(-1,1,0,0)| (X_1, X_2, X_3, X_4) }=P_1=ϕ HW$\triangle$ t+$o(\triangle$ t).

Based on the stochastic modeling technique introduced by Allen et al. [47], the system of stochastic model equations is derived and given by the following expressions.

$$\left.\begin{aligned} d\vec{X} &= \vec{f}(t, \vec{X}(t))dt + B(t, \vec{X}(t))d\vec{W}(t) \\ \vec{X}(0) &= [X_1(0), X_2(0), X_3(0), X_4(0)]^T \end{aligned}\right\}.$$

Here we define the drift vector as

$$\vec{f} = \sum_{j=1}^{13} P_j \vec{\lambda}_j. \tag{27}$$

Here, $\vec{\lambda}_j$ represents the random changes, and P_j denotes the corresponding transition probabilities (refer to Table 2).
The drift vector $\vec{f}$ is given by

$$\vec{f} = P_1\vec{\lambda}_1 + P_2\vec{\lambda}_2 + P_3\vec{\lambda}_3 + P_4\vec{\lambda}_4 + P_5\vec{\lambda}_5 + P_6\vec{\lambda}_6 + P_7\vec{\lambda}_7 + P_8\vec{\lambda}_8 + P_9\vec{\lambda}_9 + P_{10}\vec{\lambda}_{10} + P_{11}\vec{\lambda}_{11} + P_{12}\vec{\lambda}_{12}, \tag{28}$$

$$\vec{f} = \begin{bmatrix} rX_1\left(1 - \frac{X_1+X_2}{s}\right) - \frac{\phi X_1 X_2}{1+\gamma X_3} \\ \frac{\phi X_1 X_3}{1+\gamma X_3} - kX_1 - bX_4 \\ \alpha X_1 - \mu X_3 - vX_4X_3 \\ \delta + \beta X_1 - \xi X_4 \end{bmatrix}. \tag{29}$$

We shall derive the covariance matrix which is defined as

$$\vec{B} = \begin{pmatrix} V_{11} & V_{12} & 0 & V_{14} \\ V_{21} & V_{22} & 0 & 0 \\ 0 & 0 & V_{33} & 0 \\ V_{41} & 0 & 0 & V_{44} \end{pmatrix}, \tag{30}$$

where,

$$V_{11} = P_1 + P_5 + P_{10} + P_{11} + P_8 = \phi X_1 X_3 + \gamma X_1 X_3^2 + rX_1 + \frac{rX_1(X_1+X_2)}{s} + \mu X_3,$$

$V_{22} = P_1 + P_2 + P_4 = \phi X_1 X_3 + kX_2 + bX_4 X_2,$

$V_{33} = P_3 + P_8 = \alpha X_2 + \mu X_3,$

$V_{44} = P_6 + P_7 + P_9 = \delta + \beta X_2 + \xi X_4,$

$V_{12} = V_{21} = -P_1 = -\phi X_1 X_3,$

$V_{14} = V_{41} = -P_8 = -\mu X_3.$

The square root of this covariance matrix must be computed. However, for an $n \times n$ positive semi - definite matrix with order greater than two, there is no explicit formula for calculating its square root. Therefore, in order to proceed, we will implement the second modeling procedure, which generates a diffusion matrix for which a square root may not be required. Following the second modeling approach developed by Allen et al. [47], the corresponding stochastic model is presented as follows.

$$d\vec{X} = \vec{f}(t, \vec{X}(t)dt + G(t, \vec{X}(t))d\vec{W}(t), \tag{31}$$

$$\vec{X}(0) = [X_1(0), X_2(0), X_3(0), X_4(0)]^T. \tag{32}$$

The drift vector $\vec{f}$ is the same as that obtained in the first modeling procedure.
The diffusion matrix G is defined by

$$G = \lambda_{i,j} P_j^{1/2}, \quad j = 1, 2, ..., 12, \quad i = 1, 2, ..., 4 \tag{33}$$

$$G = \begin{bmatrix} -\sqrt{\phi X_1 X_3} & 0 & 0 & 0 & -\sqrt{\gamma X_1 X_3^2} & 0 & 0 & 0 & 0 & \sqrt{rX_1} & -\sqrt{\frac{rX_1(X_1+X_2)}{s}} & \sqrt{\mu X_3} \\ \sqrt{\phi X_1 X_3} & -\sqrt{kX_2} & 0 & -\sqrt{bX_4 X_2} & 0 & 0 & 0 & 0 & 0 & 0 & 0 & 0 \\ 0 & 0 & \sqrt{\alpha X_2} & 0 & 0 & 0 & 0 & -\sqrt{\mu X_3} & 0 & 0 & 0 & 0 \\ 0 & 0 & 0 & 0 & 0 & \sqrt{\delta} & \sqrt{\beta X_2} & 0 & -\sqrt{\xi X_4} & 0 & 0 & -\sqrt{\mu X_3} \end{bmatrix}$$

In the SDE formulation, the diffusion matrix G encodes the stochastic fluctuations associated with each biological transition in the system. Each column of G corresponds to a specific reaction or event (e.g., infection, recovery, natural death, recruitment), while the non-zero entries indicate how that event changes the state variables. The square-root terms arise from the standard deviation of the Poisson process governing each transition rate. For example, the term $-\sqrt{\phi X_1 X_3}$ in the first row represents the random decrease in susceptibles due to infection, while the corresponding $+\sqrt{\phi X_1 X_3}$ in the second row represents the simultaneous stochastic increase in exposed individuals from the same event. In this way, G directly links the random noise terms to the underlying biological processes.

Therefore, the Itô stochastic differential model is expressed in the following way:

$$dX(t) = f(X_1, X_2, X_3, X_4)\, dt + G\, dW(t), \tag{34}$$

which can also be written as

$$dX(t) = f(t, X(t))\, dt + B(t, X(t))\, dW(t),$$

with initial conditions

$$X(0) = \big(X_1(0), X_2(0), X_3(0), X_4(0)\big)^T,$$

and

$$W(t) = \big(W_1(t), W_2(t), W_3(t), W_4(t)\big)^T$$

is denoting a vector of independent Wiener processes (standard Brownian motions) representing stochastic fluctuations. $B(t, X(t))$ is the diffusion matrix describing how these stochastic effects influence the state variables.
Therefore, the SDE model is subsequently constructed as follows:

$$\begin{aligned} dH = &\left(rH\left(1 - \frac{H+E}{s}\right) - \frac{\phi HL}{1+\gamma L}\right) dt - \sqrt{\phi X_1 X_3} dW_1 - \sqrt{\gamma X_1 X_3^2} dW_5 \\ &+ \sqrt{rX_1} dW_{10} - \sqrt{(rX_1(X_1+X_2)/s)} dW_{11} - \sqrt{\mu X_3} dW_{12}, \end{aligned} \tag{35}$$

$$dE = \left(\frac{\phi HL}{1+\gamma L} - kE - bAE\right) dt + \sqrt{\phi X_1 X_3} dW_1 - \sqrt{kX_2} dW_2 - \sqrt{bX_4 X_2} dW_4, \tag{36}$$

$$dL = (\alpha E - \mu L - vAL)\, dt + \sqrt{\alpha} dW_3 - \sqrt{\mu X_3} dW_8, \tag{37}$$

$$dA = (\delta + \beta E - \xi A)\, dt + \sqrt{\delta} dW_6 + \sqrt{\delta} dW_7 - \sqrt{\xi X_4} dW_9 - \sqrt{\mu X_3} dW_{12}. \tag{38}$$

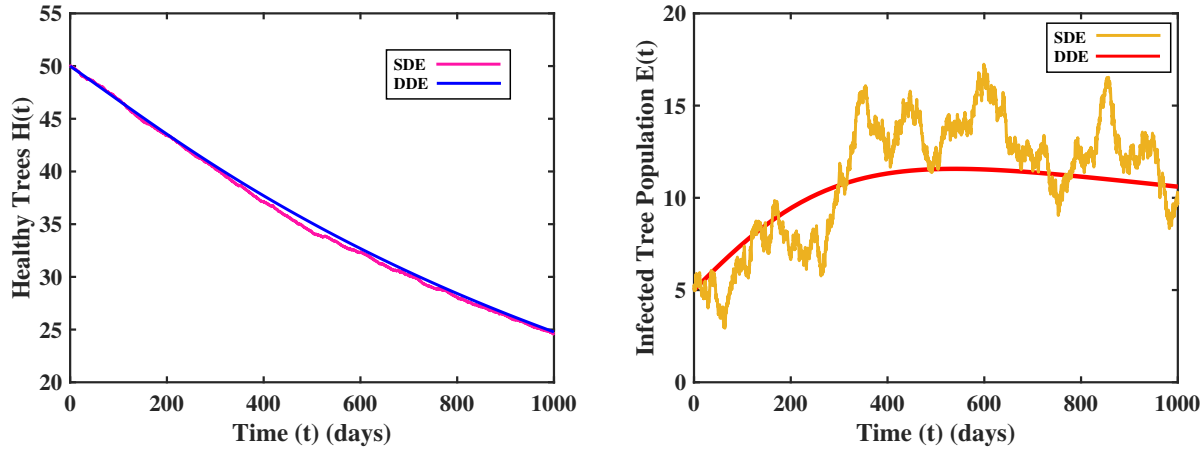

(a) (b)

Figure 7: The plot illustrates the variation that investigates the difference between DDE and SDE of (a) healthy tree population, (b) infected tree population.

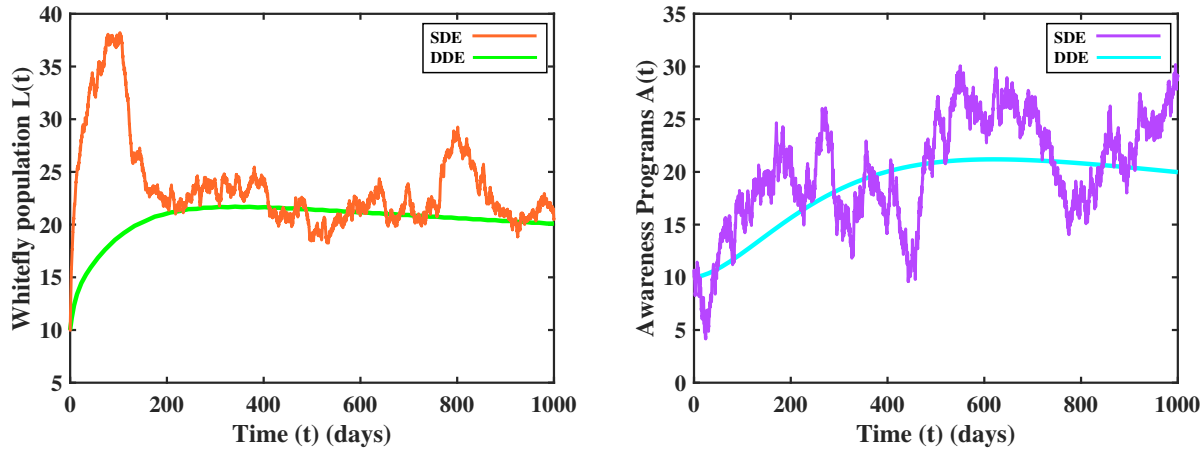

(a) (b)

Figure 8: The plot illustrates the variation that investigates the difference between DDE and SDE of (a) whitefly population, (b) awareness programs.

4. Sensitivity analysis

This Section discusses the impact of varying parameter values on the functional value of the reproduction number R_0. Since the critical parameter may act as a critical threshold for illness therapy, it must be determined [48]. The sensitivity indices of R_0 with respect to the parameters $\phi, s, \alpha, \xi, k, b, \delta, \mu, v$ are represented algebraically as follows:

$$\frac{\partial R_0}{\partial \phi} = \frac{s\alpha\xi^2}{(\xi k + b\delta)(\mu\xi + v\delta)}, \quad \frac{\partial R_0}{\partial s} = \frac{\phi\alpha\xi^2}{(\xi k + b\delta)(\mu\xi + v\delta)},$$

$$\frac{\partial R_0}{\partial \alpha} = \frac{\phi s\xi^2}{(\xi k + b\delta)(\mu\xi + v\delta)},$$

$$\frac{\partial R_0}{\partial \xi} = \frac{2\phi s\alpha\xi}{(\xi k + b\delta)(\mu\xi + v\delta)} - \frac{\phi s\alpha\xi^2 k}{(\xi k + b\delta)^2(\mu\xi + v\delta)} - \frac{\phi s\alpha\xi^2\mu}{(\xi k + b\delta)(\mu\xi + v\delta)^2},$$

$$\frac{\partial R_0}{\partial k} = \frac{-\phi s\alpha\xi^3}{(\xi k + b\delta)^2(\mu\xi + v\delta)}, \quad \frac{\partial R_0}{\partial b} = \frac{-\phi s\alpha\xi^2\delta}{(\xi k + b\delta)^2(\mu\xi + v\delta)},$$

$$\frac{\partial R_0}{\partial \delta} = \frac{-\phi s\alpha\xi^2 b}{(\xi k + b\delta)^2(\mu\xi + v\delta)} - \frac{\phi s\alpha\xi^2 v}{(\xi k + b\delta)(\mu\xi + v\delta)^2},$$

$$\frac{\partial R_0}{\partial \mu} = \frac{-\phi s\alpha\xi^3}{(\xi k + b\delta)(\mu\xi + v\delta)^2}, \quad \frac{\partial R_0}{\partial v} = \frac{-\phi s\alpha\xi^2\delta}{(\xi k + b\delta)(\mu\xi + v\delta)^2}.$$

The analysis concludes that certain partial derivatives are positive, and that increasing any of the positive parameters ϕ, s, α, ξ causes an increase in the basic reproductive number R_0. Elasticity is estimated by assessing the proportional response to proportional perturbations. We've

$$E_\phi = \frac{\phi}{R_0}\frac{\partial R_0}{\partial \phi} = \left(\frac{\phi(\xi k + b\delta)(\mu\xi + v\delta)}{\phi s\alpha\xi^2}\right)\left(\frac{s\alpha\xi^2}{(\xi k + b\delta)(\mu\xi + v\delta)}\right) = 1,$$

$$E_s = \frac{s}{R_0}\frac{\partial R_0}{\partial s} = \left(\frac{s(\xi k + b\delta)(\mu\xi + v\delta)}{\phi s\alpha\xi^2}\right)\left(\frac{\phi\alpha\xi^2}{(\xi k + b\delta)(\mu\xi + v\delta)}\right) = 1,$$

$$E_\alpha = \frac{\alpha}{R_0}\frac{\partial R_0}{\partial \alpha} = \left(\frac{\alpha(\xi k + b\delta)(\mu\xi + v\delta)}{\phi s\alpha\xi^2}\right)\left(\frac{\phi s\xi^2}{(\xi k + b\delta)(\mu\xi + v\delta)}\right) = 1,$$

$$E_\xi = \frac{\xi}{R_0}\frac{\partial R_0}{\partial \xi}$$

$$= \frac{\xi(\xi k + b\delta)(\mu\xi + v\delta)}{\phi s\alpha\xi^2} \cdot \frac{\phi s\alpha\xi}{(\xi k + b\delta)(\mu\xi + v\delta)}\left(2 - \frac{\xi k}{\xi k + b\delta} - \frac{\xi\mu}{\mu\xi + v\delta}\right)$$

$= 0.6428.$

E_ϕ, E_s, E_α, and E_ξ are all positive, as evidenced by the above expressions. This indicates that an increase in the values of the parameters ϕ, s, α, ξ leads to an increase in the basic reproduction number R_0. The fundamental reproduction number can experience

significant variation from even the smallest alterations in these parameters. It is essential to precisely calculate sensitive parameters, as minor changes can cause major quantitative changes in the system.

Figure 9: Coconut trees

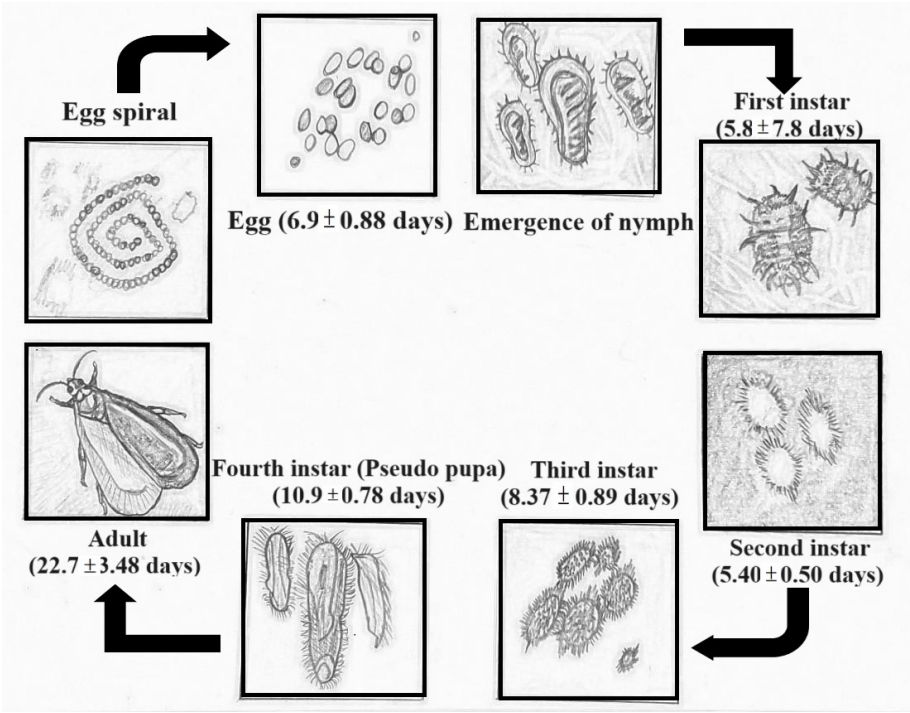

Figure 10: Life cycle of Rugose Spiralling Whitefly

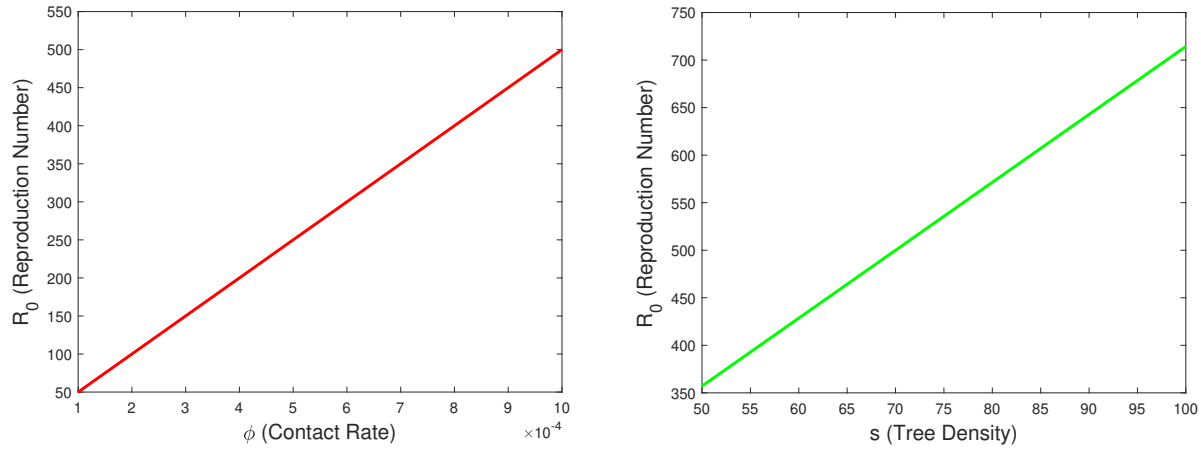

(a) (b)

Figure 11: The plot illustrates reproduction number corresponding to the sensitive parameter (a) ϕ, (b) s.

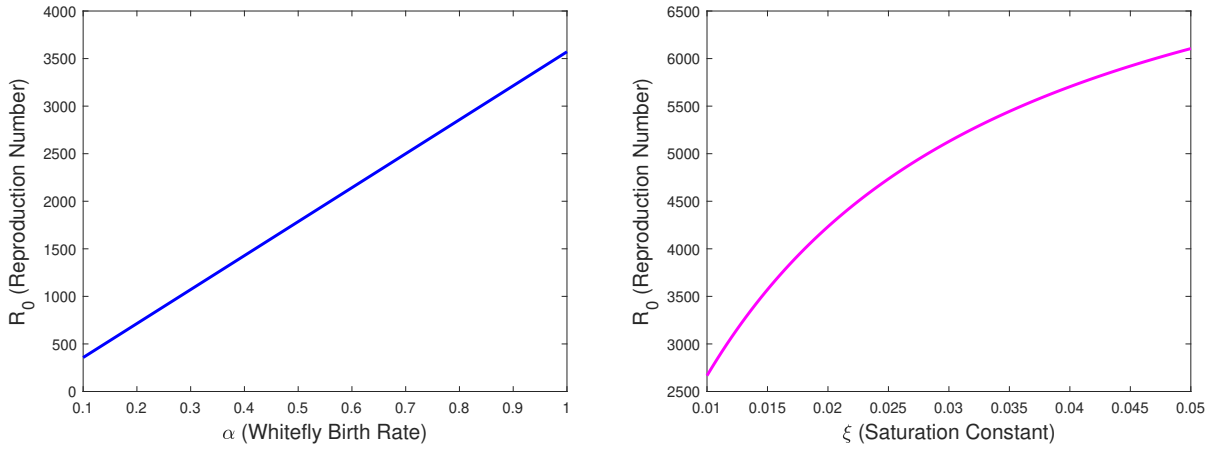

(a) (b)

Figure 12: The plot illustrates reproduction number corresponding to the sensitive parameter (a) α, (b) ξ.

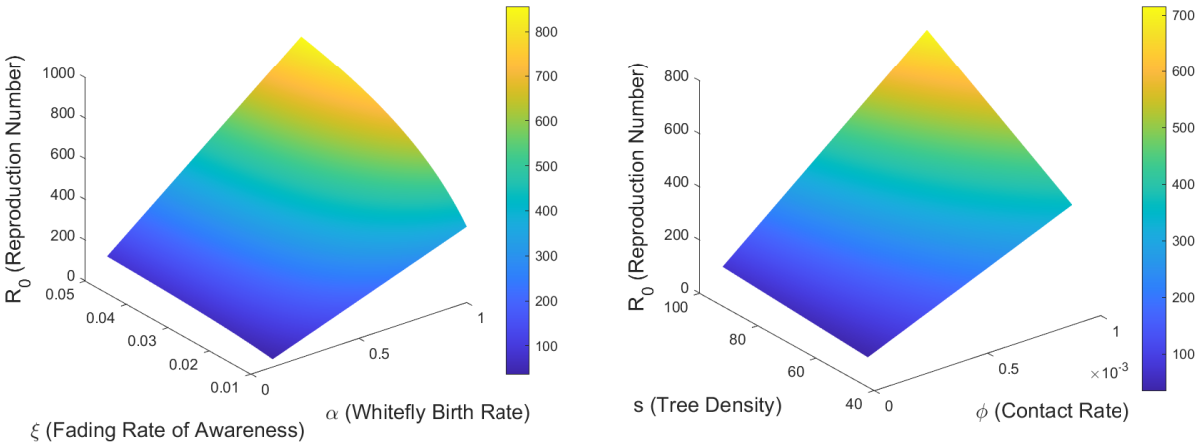

Figure 13: Surface plot illustrating the reproduction number R_0 in relation to (a) ξ and α, (b) s and ϕ.

5. Results and discussion

We have selected the values in a manner that allows numerical analysis to be performed using a reference point for each parameter. We consider an initial population of 50 healthy trees, 5 infected trees, 10 whiteflies per tree, and 10 awareness programs. So, we start with the following initial values for $H(0) = 50$, $E(0) = 5$, $L(0) = 10$, and $A(0) = 10$. Figure 1 displays the schematic diagram of our model.

Figure 2a shows the variation of $H(t)$ with different contact rates ϕ while keeping $\tau = 0.5$ fixed. As ϕ increased, the rate at which healthy trees became infected, leading to a more rapid decline in the healthy tree population. Figure 2b depicts the variation of $H(t)$ with different replanting rates r. Higher values of r counteracted the loss of healthy trees by replacing infected ones, resulting in a slower decline in $H(t)$. Figure 3a shows the effect of varying the contact rate ϕ on $E(t)$. An increase in ϕ accelerated the infection process, causing $E(t)$ to rise to higher peak values before stabilizing. Figure 3b shows the influence of the whitefly death rate μ on $E(t)$. Larger μ values reduced the number of vectors, thereby lowering the infected tree population over time. Figure 4a demonstrates the effect of changing the time delay τ on $E(t)$. Increasing τ slightly delayed the peak of infection, with larger delays associated with a marginally higher infected tree population during the peak period. Figure 5a shows the variation in $L(t)$ for different whitefly birth rates α. Higher α values led to more rapid growth of the whitefly population and larger peak values. Figure 5b illustrates the effect of increasing the whitefly death rate μ. Larger μ values reduced both the peak and steady-state levels of $L(t)$. Figure 5c examines the influence of time delay τ, showing that longer delays caused higher peaks in $L(t)$ before reaching equilibrium. Figure 6a shows the impact of increasing the local

awareness rate β. Larger β values led to faster and higher growth of awareness programs. Figure 6b depicts the effect of the fading rate ξ. Higher ξ values decreased the maximum awareness level and accelerated its decline over time. Figure 6c presents the variation with different time delays τ, showing that increasing τ resulted in higher peaks in $A(t)$ before settling. Figure 7a compares $H(t)$ for DDE and SDE models. Both showed similar overall trends, but the SDE model captured small stochastic fluctuations around the deterministic trajectory. Figure 7b compares $E(t)$ under DDE and SDE, where the SDE results exhibited higher variability due to random effects. Figure 8a shows $L(t)$ for both models, with stochastic variation being more pronounced compared to $H(t)$ and $E(t)$. Figure 8b compares $A(t)$ between DDE and SDE, revealing noticeable fluctuations in the stochastic case. The benefit of comparing the DDE and SDE formulations was that it highlighted how stochastic fluctuations influenced system dynamics, providing deeper insights into variability, uncertainty, and the robustness of the model predictions. Figure 9 displays the picture of coconut trees taken in a coconut plantation near Pollachi, Tamil Nadu. Figure 10 displays the life cycle of rugose spiralling whitefly.

In Figure 11a, illustrates when ϕ increases, the reproduction number grows proportionally, indicating that higher contact rates between trees and whiteflies result in greater potential for whitefly infestation spread, 11b illustrates the density of trees s increases, the reproduction number also rises, indicating that higher tree densities facilitate the spread of whitefly infestations. Figure 12a it is inferred that the whitefly birth rate α rises, the basic reproduction number grows significantly, highlighting the strong influence of whitefly reproduction on the potential for infestation spread, 12b displays the higher fading rate of awareness ξ significantly influences the potential for disease or infestation spread, as a greater R_0 indicates a stronger possibility of an outbreak or epidemic. The graph shows the critical role of awareness decay in controlling the spread within a population.

Figure 13a shows that R_0 increases with both higher contact rates ϕ and greater tree density s, indicating that a higher density of trees, combined with more frequent interactions, can lead to an increase in the spread of an infestation. The color bar on the right represents the corresponding values of R_0, with warmer colors (yellow and green) denoting higher reproduction numbers. This emphasizes the role of environmental and contact factors in influencing potential outbreak dynamics. Figure 13b shows that as α increases, R_0 also rises, particularly when ξ is small. This indicates that a higher whitefly birth rate α can significantly contribute to the spread of an infestation. However, when ξ increases, representing a higher rate of awareness or intervention, the value of R_0 is mitigated, underscoring the importance of awareness in controlling the spread. The color bar on the right highlights the value of R_0, with warmer colors (yellow and green) signifying higher reproduction numbers. Table 1 shows the parameter values used for the analysis and Table 2 shows the various state changes along with their respective probabilities.

6. Conclusion

This study developed a comprehensive mathematical model using both DDEs and SDEs to analyze the complex dynamics of whitefly infestations in coconut farming. The

DDE model captured the delayed effects of awareness programs and, through equilibrium and stability analysis, demonstrated that the time delay parameter τ played a critical role in determining whether the infestation persisted or was eliminated. Numerical simulations and sensitivity analyses further showed that even moderate delays in implementing awareness programs significantly affected outbreak control. The inclusion of the SDE model addressed environmental and demographic variability, offering a more realistic representation of the system's behavior under uncertainty. This integrated approach strengthened the predictive capabilities of the model and supported the development of more resilient pest management strategies. By bridging mathematical analysis with ecological dynamics and farming interventions, this work offered detailed insights into the timing and effectiveness of awareness-based controls for pest outbreaks. By capturing both delayed responses and environmental variability, the study paved the way for more resilient and adaptive pest management.

Future research can extend this model by incorporating spatial dynamics to capture the geographical spread of infestations across plantations, as well as economic factors to optimize resource allocation for control strategies. Coupling the model with economic optimization could support cost-effective intervention planning. The inclusion of multiple pest species and natural predator–prey interactions would improve the biological realism of the framework. Furthermore, integrating real-time field data through data assimilation techniques could allow the development of adaptive, evidence-based policies that respond dynamically to emerging infestations. Such advancements would enhance the model's applicability for decision-making in sustainable agricultural pest management.

Acknowledgements

We sincerely thank the reviewers for their valuable comments, which were of great help in revising the manuscript. The authors are pleased to acknowledge the financial support of the Selective Excellence Research Initiative (SRMIST/R/AR(A)/SERI2023/174/31). It is our pleasure to thank the College of Engineering and Technology, SRM IST for its valuable support and constant encouragement.

Credit Authorship Contribution Statement

B. Dhivyadharshini: Investigation, Methodology, Software, Writing – original draft, Visualization.
R. Senthamarai: Conceptualization, Methodology, Validation, Resources, Writing – review & editing, Supervision.

Conflict of Interest

The authors declare that there is no conflict of interest.

References

[1] C.C. Sreejith, C. Muraleedharan, P. Arun, Life cycle assessment of producer gas derived from coconut shell and its comparison with coal gas: An Indian perspective. *Int. J. Energy Environ. Eng.,* 4: 1–22, 2013.

[2] A. Snehalatharani, H. P. Maheswarappa, V. Devappa, S.k. Malhotra. Status of coconut basal stem rot disease in India - A review. *Indian J. Agric. Sci.,* 86: 1519–1529, 2016.

[3] A. Varghese, J. Jacob. A study of physical and mechanical properties of the Indian coconut for efficient dehusking. *Journal of Natural Fibers*, 14(3), 390-399, 2017.

[4] F. M. Dayrit, T. N. Mary, The Potential of coconut oil and its derivatives as effective and safe antiviral agents against the novel coronavirus. *Indian Coconut Journal,* 62: 21-23, 2020.

[5] G. Suganya and R. Senthamarai. Analytical Approximation of a Nonlinear Model for Pest Control in Coconut Trees by the Homotopy Analysis Method. *Computer Research and Modeling*, 14(5): 1093–1106, 2022.

[6] B. Dhivyadharshini and R. Senthamarai. Modeling the indirect impact of rhinoceros beetle control on red palm weevils in coconut plantations. *Computer Research and Modeling,* 17(4): 737 − 752, 2025.

[7] D. Narayana, K. N. Nair, Trends in area, production and productivity of coconuts in Kerala. *Indian Journal of Agricultural Economics,* 44(902-2018-2692): 159-167, 1989.

[8] k. Nihad, A. Haris, S. Kalavathi, Scope of floriculture in coconut garden. *Indian Coconut Journal,* 5-8, 2020.

[9] J.U. Chikaire, J.O. Ajaero, C.N. Atoma, Socio-economic Effects of Covid-19 pandemic on rural farm families' well-being and food systems in Imo State, Nigeria. *Journal of Sustainability and Environmental Management,* 1(1), 18-21. 2022.

[10] M. Abad, P. Noguera, R. Puchades, A. Maquieira, V. Noguera Physico-chemical and chemical properties of some coconut coir dusts for use as a peat substitute for containerised ornamental plants. *Biores. Technol.,* 82:241-245, 2002.

[11] O. A. Carrijo, R.S. Liz, N. Makishima. Green coconut husk fiber as an agricultural substrate. *Hort. Bras.,* 20:533-535, 2002.

[12] M.U.C. Nunes. Coconut husk fiber and dust: products of great importance for industry and agriculture. In: Aragão WM (Ed.) Coconut: Post-Harvest, Embrapa Information Technology, *Brasília (Brazilian Fruit Series)*, 29:66-71, 2002.

[13] J.E.G. van Dam, M.J.A. van den Oever, E.R.P, Keijsers. Production process for high density high performance binderless boards from whole coconut husk. *Ind. Crops Prod.,* 20:97-101, 2004.

[14] S. Nadanasabapathy, R. Kumar. Physico-chemical constituents of tender coconut (Cocos nucifera) water. *The Indian J. Agric. Sci.,* 69: 750-51, 2013.

[15] J.H. Martin *Zootaxa,* 681: 1-119, 2004.

[16] K.S. Karthick, C. Chinniah, P. Parthiban, A. Ravikumar. Newer report of Rugose Spiraling Whitefly, Aleurodicus rugioperculatus Martin (Hemiptera: Aleyrodidae) in India. *International Journal of Research Studies in Zoology* 4(2), 2018, 12-16.

[17] K. Elango, S. Jeyarajan Nelson, S. Sridharan, V. Paranidharan and S. Balakrishnan. Biology, Distribution and host range of new invasive pest of India coconut rugose spiralling whitefly aleurodicus rugioperculatus martin in Tamil Nadu and the status of its natural enemies. *International Journal of Agriculture Sciences,* 11(9): 8423-8426, 2019.

[18] G. Suganya, E. Jenitta and R. Senthamarai. A study on the dynamics of pest population with biocontrol using predator, parasite in presence of awareness. *Computer Research and Modeling,* 16(3): 713-729, 2024.

[19] A. Josephrajkumar, C. Mohan, V. Krishnakumar. Parasitism induced bio-suppression of coconut whitefly in Kerala. *Kerala Karshakan e-journal,* 26-27, 2016.

[20] C. Mohan, A. Josephrajkumar, V. Hegde, V. Krishnakumar, P.B. Renjith, A.S. Anjali and P. Chowdappa. Gradient outbreak and bio- suppression of spiralling whitefly in coconut gardens in South India. *Indian Coconut Journal,* 59(8): 9-12, 2016.

[21] L.J. Allen, F. Brauer, P. Van den Driessche and J. Wu, Mathematical epidemiology. *Berlin: Springer,* 1945: 2019.

[22] M. Sivakumar and R. Senthamarai. Mathematical model of epidemics: SEIR model by using homotopy perturbation method. *AIP Conference Proceedings,* 2112(1), 2019.

[23] B. Dhivyadharshini and R. Senthamarai. Mathematical Analysis of a Non Linear Prey Predator System: Analytical Approach By HPM. *AIP Conference Proceedings,* 2516, 2022.

[24] G. Suganya and R. Senthamarai, Mathematical modeling and analysis of the effect of the rugose spiraling whitefly on coconut trees. *AIMS Mathematics,* 7(7), 13053-13073, 2022.

[25] F.A. Basir, A. Banerjee and S. Ray, Role of farming awareness in crop pest management-A mathematical model. *Journal of theoretical biology,* 461, 59-67, 2019.

[26] A. Sharma and A.K. Misra, Modeling the impact of awareness created by media campaigns on vaccination coverage in a variable population. *Journal of biological systems,* 22(02): 249-270, 2014.

[27] F. Al Basir, E. Venturino, S. Ray, P. K. Roy, Effects of awareness program for controlling mosaic disease in Jatropha curcas plantations. *Computational and Applied Mathematics,* 37:6108–6131, 2018.

[28] P. Van den Driessche and J. Watmough. Reproduction numbers and sub-threshold endemic equilibria for compartmental models of disease transmission. *Mathematical biosciences,* 180(1-2): 29-48, 2002.

[29] M. Sivakumar and R. Senthamarai. Mathematical model of epidemics: Analytical approach to SIRW model using homotopy perturbation method. *AIP Conference Proceedings,* 2277, (2020).

[30] T. Vijayalakshmi and R. Senthamarai. An analytical approach to top predator interference on the dynamics of a food chain model. *Journal of Physics: Conference Series,* 1000(1), 2018.

[31] T. Vijayalakshmi and R. Senthamarai. Application of homotopy perturbation and variational iteration methods for nonlinear imprecise prey-predator model with stability analysis. *The Journal of Supercomputing,* 78(2): 2477-2502, 2022.

[32] Y. Kuang. Delay Differential Equations with Applications in Population Dynamics. *Academic Press, Inc., New York,* 1993.

[33] R.V. Culshaw and S. Ruan. A delay-differential equation model of HIV infection of $CD4^+$ T-cells. *Mathematical Biosciences,* 165:27–39, 2000.

[34] R.A. Umana, A. Omame, S.C. Inyama, Deterministic and Stochastic Models of the Dynamics of Drug Resistant Tuberculosis. *FUTOJNLS,* 2(2): 173-194, 2016.

[35] S. Boulaaras, S. I. Araz, A. Alharbi. Radiotherapy Effects in Tumor Treatment: A Piecewise Model with Deterministic and Stochastic Approaches. *Fractals,* 16(44), 2025.

[36] S. I. Araz, M. A. Cetin, A. Atangana. Existence, uniqueness and numerical solution of stochastic fractional differential equations with integer and non-integer orders. *Electronic Research Archive,* 32(2): 733–761, 2024.

[37] İ. A. Arık, S. İ. Araz. Crossover behaviors via piecewise concept: A model of tumor growth and its response to radiotherapy. *Results in Physics,* 41: 105894, 2022.

[38] K. S. Kim, S. Kim, I. H. Jung, Dynamics of tumor virotherapy: A deterministic and stochastic model approach. *Stochastic Analysis and Applications,* 34(3): 483-495, 2016.

[39] F.A. Basir, E. Venturino, S. Ray and P.K. Roy, Impact of farming awareness and delay on the dynamics of mosaic disease in Jatropha curcas plantations. *Computational and Applied Mathematics,* 37(5), 6108-6131, 2018.

[40] G. Suganya and R. Senthamarai. Impact of Awareness on the Dynamics of Pest Control in Coconut Trees - A Mathematical Model, *Engineering Letters,* 30:4, 30(4) 2022.

[41] J. Hale. Theory of functional differential equations. Springer, *Heidelberg,* 1977.

[42] M. Bodnar. The nonnegativity of solutions of delay differential equations. *Appl Math Lett* 13(6):91–5, 2000.

[43] X. Yang, L. Chen, J. Chen. Permanence and positive periodic solution for the single species nonautonomus delay diffusive model. *Comput Math Appl,* 32:109–116, 1996.

[44] O. Diekmann, Heesterbeek JAP, and Metz JAJ. On the definition and the computation of the basic reproduction ratio R_0 in models for infectious diseases in heterogeneous populations. *Journal of Mathematical Biology*, 28(4):365–382, 1990.

[45] H.I. Freedman, V.S.H Rao, The trade-off between mutual interference and time lags in predator–prey systems. *Bull Math Biol*, 45(6):991–1004, 1983.

[46] Y. Yuan, L.J.S. Allen, Stochastic models for virus and immune system dynamics. *Math. Biosci.,* 234:84–94, 2011.

[47] E. J. Allen, L.J.S. Allen, A. Arciniega, P. E. Greenwood, Construction of equivalent stochastic differential equation models. *Stoch. Anal. Appl.,* 26(2): 274 – 297, 2008.

[48] B. Dhivyadharshini, R. Senthamarai. Modeling Rugose Spiraling Whitefly Infestation on Coconut Trees Using Delay Differential Equations: Analysis via HPM. *European Journal of Pure and Applied Mathematics,* 17(3): 1908 – 1936, 2024.